

1 **SARS-CoV-2 infection causes hyperglycaemia in cats**

2

3 Authors: Yufei Zhang^{1,2,&}; Jindong Gao^{2,&}; Kun Huang^{1,2}; Ya Zhao^{1,2}; Xianfeng Hui^{1,2};

4 Ting Wang^{1,2}; Changmin Hu¹; Xiaomei Sun^{1,2}; Ying Yang^{1,2}; Chao Wu^{1,2}; Xi Chen²;

5 Zhong Zou^{1,2}; Lian zong Zhao^{1,2}; Meilin Jin^{1,2*}

6

7 1 State Key Laboratory of Agricultural Microbiology, Huazhong Agricultural University,

8 Wuhan 430070, P.R China.

9 2 College of Veterinary Medicine, Huazhong Agricultural University, Wuhan, 430070,

10 P.R China.

11 & These authors contributed equally to this work.

12 * Corresponding author E-mail: jml8328@126.com.

13

14 **Running title:** Cats as model for hyperglycaemia with COVID-19

15 **Main point:** Cats infected with a high dose of SARS-CoV-2 exhibited signs of hyperglycaemia.

16 Furthermore, upon injection of the virus post-immunisation with inactivated SARS-CoV-2, the

17 cats did not exhibit signs of hyperglycaemia. These findings indicate that SARS-CoV-2 infection

18 causes hyperglycaemia in cats.

1 **Abstract**

2 Isolated reports of new-onset diabetes in patients with COVID-19 have led researchers to
3 hypothesise that SARS-CoV-2 infects the human exocrine and endocrine pancreatic cells
4 ex vivo and in vivo. However, existing research lacks experimental evidence indicating
5 that SARS-CoV-2 can infect pancreatic tissue. Here, we found that cats infected with a
6 high dose of SARS-CoV-2 exhibited hyperglycaemia. We also detected SARS-CoV-2
7 RNA in the pancreatic tissues of these cats, and immunohistochemical staining revealed
8 the presence of SARS-CoV-2 nucleocapsid protein (NP) in the islet cells. SARS-CoV-2
9 NP and Spike proteins were primarily detected in Glu⁺ cells, and most Glu⁺ cells
10 expressed ACE2. Additionally, immune protection experiments conducted on cats
11 showed that the blood glucose levels of immunised cats did not increase post-challenge.
12 Our data indicate the cat pancreas as a SARS-CoV-2 target and suggest that the infection
13 of Glu⁺ cells could contribute to the metabolic dysregulation observed in SARS-CoV-2-
14 infected cats.

15 **Keywords:** SARS-CoV-2, coronavirus, viruses, coronavirus disease, COVID-19, cats,
16 hyperglycaemia, islet, pancreas, diabetes.

17

1 **Introduction**

2 Coronavirus disease 19 (COVID-19), caused by a severe acute respiratory syndrome
3 coronavirus 2 (SARS-CoV-2) infection, has been declared a pandemic and continues to
4 present a serious threat to public health worldwide. As of March 2021, 458,479,635 cases
5 of COVID-19 were confirmed, and 6,047,653 patients had succumbed to the disease
6 globally. The number of cases and deaths continues to rise, and a second wave of
7 infection has been reported in certain countries that had reopened their economies.
8 Moreover, the emergence of SARS-CoV-2 variants with enhanced transmissibility,
9 pathogenesis, and resistance to vaccines presents an urgent challenge to best control the
10 COVID-19 pandemic [1-4]. Reports published to date on the COVID-19 outbreak include
11 a large quantity of data indicating the presence of a bidirectional interaction between
12 COVID-19 and diabetes. However, the mechanisms underlying this interaction remain
13 elusive [5-12]. Multiple forms of diabetes, including new-onset diabetes, and metabolic
14 complications, such as diabetic ketoacidosis and hyperosmolarity, might be observed in
15 patients with COVID-19 [6-12]. Intriguingly, emerging evidence shows that a new
16 diagnosis of diabetes is frequently observed in patients with COVID-19 and is a risk
17 factor for poor prognosis, particularly in patients with severe to critical COVID-19 [6-
18 12]. Therefore, fasting blood glucose (FBG) is an important prognostic factor in COVID-
19 19, which can be used to estimate the magnitude of association between COVID-19 and
20 diabetes. While a J-shaped association between FBG content and COVID-19 severity has
21 been reported in patients without diabetes [12], the molecular mechanism underlying the

1 relationship between COVID-19 and hyperglycemia remains unclear.

2 The precise mechanisms underpinning the development of new-onset diabetes in patients
3 with COVID-19 remain unknown, but it is likely that a number of complex, interrelated
4 etiologies are responsible, including impairments in both glucose disposal and insulin
5 secretion, stress hyperglycemia, preadmission diabetes, and steroid-induced diabetes [13,
6 14]. Previous data have demonstrated that SARS-CoV-2 triggers transient hyperglycemia
7 and impaired pancreatic β -cell function in the context of epidemic-derived pneumonia
8 [15-18]. However, evidence of ACE2 expression in pancreatic cells remains conflicting,
9 with studies pointing to ACE2 expression in a limited subset of β -cells [19].
10 Alternatively, the proinflammatory cytokines and acute-phase reactants resulting from
11 COVID-19 could directly result in inflammation and damage to pancreatic β -cells [13].
12 Moreover, the COVID-19-induced inflammation and cytokine storm (CS), which are
13 characterized by profound increases in the levels of tumor necrosis factor-alpha (TNF- α)
14 and interleukin (IL)-6, lead to peripheral insulin resistance (IR). Another study has
15 revealed that adipose dysfunction is a feature of COVID-19 that may drive
16 hyperglycemia [20]. Taken together, data suggest that IR, adipose dysfunction, and
17 impairment of pancreatic β -cell function contribute to a vicious cycle involved in the
18 development and progression of hyperglycemia in COVID-19 patients [21]. However, the
19 current study cannot address in detail the mechanisms underpinning islet impairment and
20 metabolic dysregulation. Further cellular and animal models need to be analyzed to
21 address this question.

1 Many different studies have shown that both cats and ferrets were efficiently infected and
2 could transmit the virus, and dogs showed low susceptibility [22-27]. Here, we present an
3 in-depth study of SARS-CoV-2-infection-associated disease in domestic cats.
4 Interestingly, in this study, an unexpected and abnormal increase in blood glucose levels
5 was observed in cats with SARS-CoV-2 infection under laboratory conditions.
6 Meanwhile, SARS-CoV-2 RNA and protein were detected in the pancreas of these cats.
7 In addition, we also observed the cellular localization pattern of SARS-CoV-2 in
8 pancreatic endocrine cells and explored an effective animal model for the thorough
9 investigation of the pathogenic mechanism underlying SARS-CoV-2 infection in patients
10 with new-onset diabetes.

11 **Materials and Methods**

12 **Cells and viruses**

13 SARS-CoV-2 (strain HB-01) was kindly provided by Professor Zheng-Li Shi from the
14 Wuhan Institute of Virology, Chinese Academy of Sciences^{3,19}. Vero E6 cells (ATCC[®]
15 CRL-1586[™]), used for the reproduction of SARS-CoV-2 stocks, were cultured in
16 Dulbecco's modified Eagle's medium (DMEM) supplemented with 10% foetal bovine
17 serum (FBS) and antibiotics (100 U/mL penicillin/streptomycin), and incubated at 37 °C
18 in an atmosphere with 5% CO₂. The virus was titrated using 10-fold serial dilutions in
19 Vero E6 cells. Three days after the inoculation, the cytopathic effect (CPE) was scored,
20 and the Reed-Muench formula was used to calculate the TCID₅₀ value. All experiments
21 involving SARS-CoV-2 were performed at a Biosafety Level-3 (BSL3) containment

1 laboratory at Huazhong Agricultural University [28].

2 **Experimental infection**

3 Approval was obtained from the Huazhong Agricultural University Committee on the
4 Use of Live Animals in Teaching and Research. 18 specific-pathogen-free cats (70–100
5 days) were purchased from commercial breeders. The animals were maintained in
6 standard housing facilities (Biosafety Level-2) and provided access to standard pellet
7 feed and water ad libitum until the viral challenge in the BSL3 animal facility. The cats
8 were acclimated for seven days to the BSL3 animal facility prior to experimental
9 procedures with feed and water ad libitum. Before infection, the animals were examined
10 clinically, determined to be healthy by a registered veterinarian, and placed in negative
11 pressure glove boxes.

12 To assess the replication of SARS-CoV-2, nine close relatives of the specific-pathogen-
13 free cats (70–100 days) were housed in individual biosafety isolators and divided into
14 four groups. A total of two animals from each group were assigned to three subgroups: A,
15 B, and C. These groups were inoculated with 2 mL of virus solution containing 2×10^7
16 TCID₅₀ of HB-01 isolates, respectively, with 1 mL administered intratracheally and 1 mL
17 administered intranasally. Three control cats in group D were mock-infected in an
18 identical manner with 2 mL of Vero E6 cell culture supernatant. The animals were
19 monitored daily for clinical signs. At 3, 5, and 7 dpi, the cats were euthanised by arterial
20 whole blood sampling under Dexmedetomidine 5 µg/kg and ketamine 4 mg/kg IM
21 anaesthesia. Take 0.5 mL intramuscular injection according to the volume of 1:1 mixture,

1 achieve irreversible deep anesthesia beyond the surgical period. The technique of carotid
2 artery cannulation has been described previously [29-31]. Briefly, after heparinization,
3 the ventral aspect of the neck was clipped and prepared for surgery. The right carotid
4 artery was surgically exposed. A 10F straight arterial cannula was placed retrograde in the
5 carotid artery. Heparin (400U/kg) was administered to increase activated clotting time
6 (ACT) to >480 seconds. Arterial return blood was collected after releasing the clamps on
7 the venous and arterial lines.

8 **Pathological examination**

9 The animals were necropsied according to a standard protocol involving opening of the
10 thoracic and abdominal cavities and the skull and examination of all major organs,
11 including the brain. Two animals from each group were sacrificed at 3, 5, and 7 dpi, and
12 the lungs, spleen, lymph nodes, small intestine, kidney, trachea, cerebrum, pancreas, sex
13 glands, stomach, and heart were harvested from each animal. The tissues were fixed in
14 4% paraformaldehyde phosphate (PFA) buffer solution for 48 h and then processed for
15 paraffin embedding. The nasal samples were immersed in EDTA solution for
16 decalcification after fixation in PFA. The paraffin blocks were cut into sections with a
17 thickness of 4 μm and mounted on silane-coated glass slides. The tissues sections were
18 stained using haematoxylin and eosin. The histopathological changes in the different
19 tissues were observed under an Olympus microscope (Olympus, Tokyo, Japan).

20 **Challenge assay in cats**

21 Nine cats were used for evaluating the toxicity and immunogenicity of the inactivation

1 viruses. Alum, a common adjuvant, was administered at 0.45 mg/dose for animal
2 immunisation, and the alum-buffer served as the negative control. All cats were
3 immunised at days 0, 14. A challenge study was conducted 24 days after the second
4 round of immunisation by directly inoculating 2 mL of 10^7 TCID₅₀ of SARS-CoV-2 (1
5 mL administered intratracheally and 1 mL administered intranasally). Cats were observed
6 daily for clinical signs, such as: fever, anorexia, lethargy, respiratory distress,
7 inappetence, coughing, sneezing, diarrhea and vomiting. These general symptoms in the
8 animals were monitored and recorded each day during the experiment. Blood and serum
9 were collected from all cats, on days 3-, 5- and 7-day post challenge (DPC) via arterial
10 catheterization of the carotid artery under anesthesia. Euthanasia was carried out as
11 described above. A full postmortem examination was performed for each cat at the
12 indicated time-points and gross changes (if any) were recorded. Tissues were collected
13 either in 10% neutral-buffered formalin, and as fresh tissues which were used to measure
14 the viral load. Fresh frozen tissue homogenates were prepared by thawing frozen tissue
15 and placing 200 mg (\pm 50 mg) of minced tissue in a tube containing 1 mL DMEM
16 culture medium and a steel bead (Hubei Xinzongke viral Disease Control Bio-Tech).
17 Homogenization was performed with the TissueLyser LT (Hubei Xinzongke viral Disease
18 Control Bio-Tech) for 30 seconds at 30 hertz repeated 3 times. Supernatant was retained
19 after centrifugation for RNA extraction and quantitative reverse transcription real-time
20 PCR (RT-qPCR).

21

1 **Quantification and statistical analysis**

2 Data were subjected to the student's t-test using PRISM™ 8.0.2 for Windows (GraphPad
3 Software Inc., San Diego, CA, USA). Data are expressed as mean ± SEM, unless stated
4 otherwise. The displayed graphs were generated using GraphPad Prism or R. $P \leq 0.05$
5 was considered statistically significant. All experiments were repeated for three
6 biological replicates.

7 Detailed methods are provided in the Supplementary Materials.

8 **Results**

9 To assess the replication and pathogenicity of SARS-CoV-2 in cats, nine cats (70–100-
10 day old) were divided into the infection and control groups. The cats in the infection
11 group were inoculated with 2 mL of a solution containing the HB-01 strain at 2×10^7
12 median tissue culture infectious dose (TCID₅₀)/mL, with 1 mL administered
13 intratracheally and 1 mL administered intranasally (Figure 1A). The cats in the control
14 group were mock infected with 2 mL of Vero E6 cell culture supernatant following the
15 same procedures. Thereafter, the clinical symptoms of the animals were monitored for 7
16 days; the infected animals did not show any obvious clinical symptoms. On days 3, 5, and
17 7 post infection, two infected cats and one mock-infected cat were euthanized for sample
18 collection. Viral nucleic acid was detected, and pathological changes in the heart, liver,
19 spleen, lungs, kidneys, brain, intestine, and testes (male cats) were observed
20 (Supplementary Figure S1). The turbinates, tracheae, bronchi, and all lobes of the lungs
21 of the infected cats showed the presence of viral RNA at 3, 5, and 7 days post infection

1 (dpi) (Figure 1B). The viral RNA load in the lung tissues was marginally lower than that
2 in the upper respiratory tract (Figure 1B). Notably, the pancreatic tissues of all infected
3 cats tested positive for viral RNA at 5 and 7 dpi (Figure 1B), whereas the liver, spleen,
4 kidney, testis, and heart tissues did not (Figure 1B). In addition, viral titer measurement
5 indicated that the infectious viruses proliferated in the turbinates, tracheae, and lung
6 tissues but not in the small intestine, pancreas, heart, liver, spleen, kidneys, brain, and
7 submaxillary lymph nodes (Supplementary Figure S2).

8 Based on the viral RNA expression in the pancreatic tissues of all infected cats at 5 and 7
9 dpi, we hypothesized that the pancreas represented a potential target organ affected by
10 SARS-CoV-2 infection. The pancreas is a critical organ that controls the blood glucose
11 content. To assess whether SARS-CoV-2 could influence glucose metabolism, we
12 measured the blood glucose concentration of the cats before and after viral inoculation.
13 We observed that almost all SARS-CoV-2-infected cats exhibited hyperglycemia (except
14 cats #7-1, SARS-CoV-2-infected a cat at 7 dpi), whereas the cats in the control group did
15 not exhibit hyperglycemia (Figure 1C). This indicated a positive correlation between
16 SARS-CoV-2 infection and blood glucose levels. However, microscopic examination and
17 observation of the anatomopathological features indicated that SARS-CoV-2 infection
18 induced no visible pathological changes in the pancreas of the cats, and the islets were
19 clearly observable upon microscopic examination without the presence of diseased or
20 abnormal cells (Figure 1D). Immunohistochemical staining indicated the expression of
21 the SARS-CoV-2 nucleocapsid protein (NP) in the pancreatic islet cells isolated from

1 infected cats (Figure 1E). As expected, the SARS-CoV-2 NP was detected in the
2 turbinates, soft palates, tracheae, bronchioles, and alveolar epithelial cells of the infected
3 cats (Supplementary Figure S3A). However, it was not detected in the liver, kidney, and
4 brain tissue samples (Supplementary Figure S3D). Notably, SARS-CoV-2 NP expression
5 in the pancreatic tissues increased with the increase in infection time (Supplementary
6 Figure S3B and 3C). Additionally, immunohistochemical staining clearly indicated that
7 the SARS-CoV-2 NP was expressed in pancreatic ductal epithelial cells (Supplementary
8 Figure S4A). The above results strongly suggest that SARS-CoV-2 can invade the islet
9 cells and pancreatic ductal epithelial cells of cats.

10 The mechanism of virus entry is not completely clear at this point, as expression patterns
11 of the SARS-CoV-2 entry gene ACE2 in the cells of the cat endocrine and exocrine
12 pancreas remain unknown. Therefore, we performed immunohistochemical triple staining
13 for the viral N protein, glucagon, and insulin, and observed a high number of viral NP-
14 glucagon double-positive cells but only a few viral NP-insulin double-positive cells
15 (Figure 2A1-4). Likewise, similar results were identified when spike protein-specific
16 antibodies were used (Figure 2B1-4). Additionally, we performed immunohistochemical
17 triple staining for viral NP, glucagon, and ACE2, and observed a high number of triple-
18 positive cells (Figure 2C1-4). Pancreatic tissue isolated from uninfected cats did not show
19 immunopositivity for SARS-CoV-2 NP (Figure 2D1-4). In conclusion, pancreatic SARS-
20 CoV-2 infection, including that in the exocrine and endocrine cells, can occur in cats
21 infected with a high SARS-CoV-2 load.

1 To further assess the pathophysiological mechanism underlying SARS-CoV-2-induced
2 blood glucose elevation in cats, we evaluated islet cell apoptosis. We performed a
3 terminal deoxynucleotidyl transferase dUTP nick end labeling assay on the pancreatic
4 tissues, observing as such that a few pancreatic ductal epithelial cells and fewer number
5 of islet cells had undergone apoptosis (Supplementary Figure S4). Almost no apoptotic
6 cells were detectable in sections of pancreatic tissue in three of the six infected cats (cat
7 #3-1, cat #3-2, cat #5-2) or the three uninfected cats. We suggest two possible reasons
8 supporting this result. First, normal tissue could not be clearly differentiated from
9 pathologic tissue. Second, the sample size could have been too small. Finally, we
10 analyzed SARS-CoV-2-infected cat serum for the presence of insulin. The results showed
11 that serum insulin was maintained at normal levels across all experimental animals
12 (Supplementary Figure S5). The healthy cat has a fasting insulin concentration range of
13 0.713-15.065 mU/L [32, 33]. It was not difficult to see that the SARS-CoV-2-infected cat
14 serum insulin concentrations in hyperglycemic steady states were inhibited
15 (Supplementary Figure S5). This finding may potentially be explained by the decreased
16 pancreatic β -cell secretory capacity. However, the detailed mechanisms warrant further
17 investigation in the context of future studies.

18 Furthermore, we measured the cytokine levels in both the sera and lung tissues of SARS-
19 CoV-2-infected cats; various cytokines were found to be upregulated in the lung tissues
20 after SARS-CoV-2 infection (Supplementary Figure S6A). Notably, the expression of IL-
21 6 increased by more than 100 times compared to that in control cats. Consistently, the

1 levels of serum cytokines, including interferon γ , IL-1 β , IL-10, and IL-12P40 were
2 elevated in infected cats (Supplementary Figure S6B-J). These results indicated that cats
3 with SARS-CoV-2 infection experienced CS.

4 To confirm whether SARS-CoV-2 causes hyperglycemia in cats, we further performed a
5 vaccine protective experiment (Figure 3A). Six domestic kittens were immunized three
6 times with inactivated SARS-CoV-2. For control, three domestic kittens were immunized
7 with the culture medium of Vero cells under the same conditions. Following the three
8 rounds of immunization, we found that the serum neutralizing antibody titer in the
9 immunized cats was as high as 1:640 (Figure 3B). Subsequently, we challenged the
10 immunized and control cats with the virus at 2×10^7 TCID₅₀/mL, with 1 mL administered
11 intratracheally and 1 mL administered intranasally. At 3, 5, and 7 dpi, the cats were
12 euthanized and the samples were collected. The RT-qPCR results showed a lower viral
13 load in immunized cats than in control cats (Supplementary Figure S7). In addition, the
14 pancreatic tissue of immunized cats tested negative for SARS-CoV-2 nucleic acid
15 (Supplementary Figure S6). Similarly, the blood glucose levels of the challenged cats
16 were not altered significantly post immunization. However, the blood glucose levels of
17 the cats in the control group increased significantly (Figure 3C). In conclusion, SARS-
18 CoV-2 infection most likely contributed to the increase in the blood glucose levels of
19 infected cats.

20 **Discussion**

21 For many years, clinical, epidemiological, pathological, and in vitro studies have

1 implicated enteroviruses as initiators of autoimmunity and β -cell failure in genetically
2 susceptible individuals [34, 35]. Whether or not SARS-CoV-2 is also a diabetogenic virus
3 initiating the direct destruction of β -cells, thereafter leading to dysregulated endocrine
4 dynamics in the pancreas, remains up to debate. A significant number of reported SARS-
5 CoV-2 infects and replicates in cells of the human endocrine and exocrine pancreas [15,
6 17, 18, 34, 36, 37].

7 ACE2 is the key entry receptor for SARS-CoV-2. However, ACE2 is widely expressed in
8 other organs, such as the heart, kidney, gut, and pancreas [34, 38]. Multiple independent
9 laboratories have probed whether the canonical SARS-CoV-2 cell-entry machinery is
10 present in human pancreatic cells, resulting in many studies that did find pancreatic islet
11 ACE2 expression [34, 38]. This finding was consistent with data obtained from our
12 preliminary study. However, Wu and colleagues reported SARS-CoV-2 infection mainly
13 in INS+ cells [36]. In this study, we demonstrated SARS-CoV-2 infection mainly in Glu+
14 cells of the cat endocrine pancreas. These findings conflict to a certain degree with
15 previously published results. Nevertheless, it is worth clarifying two points. For one, this
16 may reflect species-specific differences. Second, the expression of ACE2 expression
17 varies across different species. Charlotte Steenblock and colleagues reported that 70% of
18 COVID-19 patients expressed ACE2 in their vasculature, while only 30% displayed
19 ACE2 expression in beta cells [15]. However, we found ACE2 expression mainly in Glu+
20 cells of the cat endocrine pancreas (Figure 2C1-4). Similar observations have also been
21 reported elsewhere. Tang and colleagues reported that SARS-CoV-2 viral RNAs,

1 including SARS-CoV-2-E, SARS-CoV-2-M, SARS-CoV-2-ORF1ab, SARS-CoV-2-
2 ORF8, SARS-CoV-2-ORF10, and SARS-CoV-2-S, were highly expressed in acinar cells,
3 alpha cells, beta cells, ductal cells, and fibroblasts in the SARS-CoV-2-infected condition
4 but not in the context of the mock-infected condition [16]. Although we believe these
5 results are of major interest, further studies with a higher number of subjects will help
6 confirm or refute our findings.

7 Previous data have demonstrated that the COVID-19-induced inflammation and CS,
8 which are characterized by strong increases in the levels of TNF- α and IL-6, lead to
9 peripheral IR [39]. Besides, high TNF- α and IL-6 in CS impair pancreatic β -cell function
10 and inhibit insulin secretion. As such, both IR and impairment of pancreatic β -cell
11 function contribute to a vicious cycle in the development and progression of
12 hyperglycemia in COVID-19 patients [21, 39]. Therefore, we speculated that the elevated
13 blood glucose content in SARS-CoV-2-infected cats may be a manifestation of metabolic
14 disorders caused by inflammation and CS.

15 However, to date, there is lack of information from detailed investigations of pancreatic
16 tissues from fatal COVID-19 cases. Therefore, whether there are pathological changes in
17 the pancreas of patients with COVID-19 and whether the pancreas is a target organ of
18 SARS-CoV-2 remains unknown [18, 40-45]. Only a thorough investigation of the
19 histopathology of the pancreas, carefully controlled in vitro infection studies, animal
20 models to directly assess the ability of SARS-CoV-2 to infect the endocrine pancreas,
21 and, most importantly, a balanced evaluation of emerging and future epidemiological
22 studies [18, 43-45] can provide us with a complete framework for the informed

1 assessment of diabetes-associated risk of COVID-19 and shed light on potential
2 intervention strategies for SARS-CoV-2 infections.

3 **Conclusions**

4 In the current study, we found that SARS-CoV-2 RNA and protein are detectable in the
5 pancreatic tissues of cats after viral inoculation, and viral inoculation can induce an
6 increase in the blood glucose levels. Cats immunized with the inactivated virus were
7 resistant to subsequent infection and hyperglycemia. We believe that these data provide
8 important insights, shedding light on the possibility that pancreatic SARS-CoV-2
9 infection can lead to hyperglycemia. Our results also point to the utility of cats as model
10 animals for the study of the molecular mechanisms underlying blood glucose regulation
11 in individuals infected with SARS-CoV-2.

12 **Notes**

13 *Acknowledgments.*

14 We thank biosafety level 3 (BSL3) facility and State Key Laboratory of Agricultural
15 Microbiology in Huazhong Agricultural University. State Key Laboratory of Virology
16 and National Virus Resource Center in Wuhan Institute of Virology, Chinese Academy of
17 Sciences for providing Wuhan-Hu-1 virus.

18 *Financial support.*

19 This research was funded by Emergency Science and Technology Project of Hubei
20 Province (2020FCA046) and Independent Science and Technology Innovation Fund of
21 Huazhong Agricultural University in 2020 (2662020PY002).

22 *Potential conflicts of interest.*

23 All other authors report no potential conflicts. All authors have submitted the ICMJE
24 Form for Disclosure of Potential Conflicts of Interest. Conflicts that the editors consider
25 relevant to the content of the manuscript have been disclosed.

1 **References**

- 2 1. Davies NG, Jarvis CI, Group CC-W, et al. Increased mortality in community-tested cases of
3 SARS-CoV-2 lineage B.1.1.7. *Nature* **2021**; 593:270-4.
- 4 2. Zhou D, Dejnirattisai W, Supasa P, et al. Evidence of escape of SARS-CoV-2 variant B.1.351 from
5 natural and vaccine-induced sera. *Cell* **2021**; 184:2348-61 e6.
- 6 3. Garcia-Beltran WF, Lam EC, St Denis K, et al. Multiple SARS-CoV-2 variants escape
7 neutralization by vaccine-induced humoral immunity. *Cell* **2021**; 184:2523.
- 8 4. Firestone MJ, Lorentz AJ, Meyer S, et al. First Identified Cases of SARS-CoV-2 Variant P.1 in the
9 United States - Minnesota, January 2021. *MMWR Morb Mortal Wkly Rep* **2021**; 70:346-7.
- 10 5. Singh AK, Gupta R, Ghosh A, Misra A. Diabetes in COVID-19: Prevalence, pathophysiology,
11 prognosis and practical considerations. *Diabetes Metab Syndr* **2020**; 14:303-10.
- 12 6. Apicella M, Campopiano MC, Mantuano M, Mazoni L, Coppelli A, Del Prato S. COVID-19 in
13 people with diabetes: understanding the reasons for worse outcomes. *Lancet Diabetes*
14 *Endocrinol* **2020**; 8:782-92.
- 15 7. Sathish T, Chandrika Anton M. Newly diagnosed diabetes in patients with mild to moderate
16 COVID-19. *Diabetes Metab Syndr* **2021**; 15:569-71.
- 17 8. Sathish T, Kapoor N, Cao Y, Tapp RJ, Zimmet P. Proportion of newly diagnosed diabetes in
18 COVID-19 patients: A systematic review and meta-analysis. *Diabetes Obes Metab* **2021**; 23:870-
19 4.
- 20 9. Bornstein SR, Rubino F, Khunti K, et al. Practical recommendations for the management of
21 diabetes in patients with COVID-19. *Lancet Diabetes Endocrinol* **2020**; 8:546-50.

- 1 10. Rubino F, Amiel SA, Zimmet P, et al. New-Onset Diabetes in Covid-19. *N Engl J Med* **2020**;
2 383:789-90.
- 3 11. Aabdi M, Aarab A, Es-Saad O, Malki K, Bkiyar H, Housni B. New-Onset Diabetes in Children
4 during COVID-19: Clinical Case Report. *Case Rep Endocrinol* **2021**; 2021:6654019.
- 5 12. Unsworth R, Wallace S, Oliver NS, et al. New-Onset Type 1 Diabetes in Children During
6 COVID-19: Multicenter Regional Findings in the U.K. *Diabetes Care* **2020**; 43:e170-e1.
- 7 13. Khunti K, Del Prato S, Mathieu C, Kahn SE, Gabbay RA, Buse JB. COVID-19, Hyperglycemia,
8 and New-Onset Diabetes. *Diabetes Care* **2021**; 44:2645-55.
- 9 14. Gazzaruso C, Coppola A, Gallotti P, Terruzzi I, Montalcini T, Luzi L. Comment on Khunti et al.
10 COVID-19, Hyperglycemia, and New-Onset Diabetes. *Diabetes Care* 2021;44:2645-2655.
11 *Diabetes Care* **2022**; 45:e45.
- 12 15. Steenblock C, Richter S, Berger I, et al. Viral infiltration of pancreatic islets in patients with
13 COVID-19. *Nat Commun* **2021**; 12:3534.
- 14 16. Tang X, Uhl S, Zhang T, et al. SARS-CoV-2 infection induces beta cell transdifferentiation. *Cell*
15 *Metab* **2021**; 33:1577-91 e7.
- 16 17. Yang L, Han Y, Nilsson-Payant BE, et al. A Human Pluripotent Stem Cell-based Platform to
17 Study SARS-CoV-2 Tropism and Model Virus Infection in Human Cells and Organoids. *Cell Stem*
18 *Cell* **2020**; 27:125-36 e7.
- 19 18. Muller JA, Gross R, Conzelmann C, et al. SARS-CoV-2 infects and replicates in cells of the
20 human endocrine and exocrine pancreas. *Nat Metab* **2021**; 3:149-65.
- 21 19. Atkinson MA, Powers AC. Distinguishing the real from the hyperglycaemia: does COVID-19

- 1 induce diabetes? *Lancet Diabetes Endocrinol* **2021**; 9:328-9.
- 2 20. Reiterer M, Rajan M, Gomez-Banoy N, et al. Hyperglycemia in acute COVID-19 is
3 characterized by insulin resistance and adipose tissue infectivity by SARS-CoV-2. *Cell Metab*
4 **2021**; 33:2174-88 e5.
- 5 21. Mehta P, McAuley DF, Brown M, et al. COVID-19: consider cytokine storm syndromes and
6 immunosuppression. *Lancet* **2020**; 395:1033-4.
- 7 22. Shi J, Wen Z, Zhong G, et al. Susceptibility of ferrets, cats, dogs, and other domesticated
8 animals to SARS-coronavirus 2. *Science* **2020**; 368:1016-20.
- 9 23. Zhang Q, Zhang H, Gao J, et al. A serological survey of SARS-CoV-2 in cat in Wuhan. *Emerg*
10 *Microbes Infect* **2020**; 9:2013-9.
- 11 24. Fernandez-Barat L, Lopez-Aladid R, Torres A. The value of serology testing to manage SARS-
12 CoV-2 infections. *Eur Respir J* **2020**; 56.
- 13 25. Segales J, Puig M, Rodon J, et al. Detection of SARS-CoV-2 in a cat owned by a COVID-19-
14 affected patient in Spain. *Proc Natl Acad Sci U S A* **2020**; 117:24790-3.
- 15 26. Barrs VR, Peiris M, Tam KWS, et al. SARS-CoV-2 in Quarantined Domestic Cats from COVID-19
16 Households or Close Contacts, Hong Kong, China. *Emerg Infect Dis* **2020**; 26:3071-4.
- 17 27. Garigliany M, Van Laere AS, Clercx C, et al. SARS-CoV-2 Natural Transmission from Human to
18 Cat, Belgium, March 2020. *Emerg Infect Dis* **2020**; 26:3069-71.
- 19 28. Zhang Y, Huang K, Wang T, et al. SARS-CoV-2 rapidly adapts in aged BALB/c mice and induces
20 typical pneumonia. *J Virol* **2021**.
- 21 29. Brouman JD, Schertel ER, Holt DW, Olshove VA. Cardiopulmonary bypass in the cat. *Vet Surg*

- 1 **2002**; 31:412-7.
- 2 30. Uechi M, Harada K, Mizukoshi T, et al. Surgical closure of an atrial septal defect using
3 cardiopulmonary bypass in a cat. *Vet Surg* **2011**; 40:413-7.
- 4 31. Borenstein N, Gouni V, Behr L, et al. Surgical Treatment of Cor Triatriatum Sinister in a Cat
5 Under Cardiopulmonary Bypass. *Vet Surg* **2015**; 44:964-9.
- 6 32. Strage EM, Holst BS, Nilsson G, Jones B, Lilliehook I. Validation of an enzyme-linked
7 immunosorbent assay for measurement of feline serum insulin. *Vet Clin Pathol* **2012**; 41:518-28.
- 8 33. Strage EM, Ley CJ, Forkman J, et al. Homeostasis model assessment, serum insulin and their
9 relation to body fat in cats. *BMC Vet Res* **2021**; 17:34.
- 10 34. Geravandi S, Mahmoudi-Aznavah A, Azizi Z, Maedler K, Ardestani A. SARS-CoV-2 and
11 pancreas: a potential pathological interaction? *Trends Endocrinol Metab* **2021**; 32:842-5.
- 12 35. Geravandi S, Liu H, Maedler K. Enteroviruses and T1D: Is It the Virus, the Genes or Both
13 which Cause T1D. *Microorganisms* **2020**; 8.
- 14 36. Wu CT, Lidsky PV, Xiao Y, et al. SARS-CoV-2 infects human pancreatic beta cells and elicits
15 beta cell impairment. *Cell Metab* **2021**; 33:1565-76 e5.
- 16 37. Shahrudin SH, Wang V, Santos RS, et al. Deleterious Effects of SARS-CoV-2 Infection on
17 Human Pancreatic Cells. *Front Cell Infect Microbiol* **2021**; 11:678482.
- 18 38. Hikmet F, Mear L, Edvinsson A, Micke P, Uhlen M, Lindskog C. The protein expression profile
19 of ACE2 in human tissues. *Mol Syst Biol* **2020**; 16:e9610.
- 20 39. Al-Kuraishy HM, Al-Gareeb AI, Alblihed M, Guerreiro SG, Cruz-Martins N, Batiha GE. COVID-
21 19 in Relation to Hyperglycemia and Diabetes Mellitus. *Front Cardiovasc Med* **2021**; 8:644095.

- 1 40. Kusmartseva I, Wu W, Syed F, et al. Expression of SARS-CoV-2 Entry Factors in the Pancreas of
2 Normal Organ Donors and Individuals with COVID-19. *Cell Metab* **2020**; 32:1041-51 e6.
- 3 41. Coate KC, Cha J, Shrestha S, et al. SARS-CoV-2 Cell Entry Factors ACE2 and TMPRSS2 Are
4 Expressed in the Microvasculature and Ducts of Human Pancreas but Are Not Enriched in beta
5 Cells. *Cell Metab* **2020**; 32:1028-40 e4.
- 6 42. Accili D. Can COVID-19 cause diabetes? *Nat Metab* **2021**; 3:123-5.
- 7 43. DiMeglio LA, Albanese-O'Neill A, Munoz CE, Maahs DM. COVID-19 and Children With
8 Diabetes-Updates, Unknowns, and Next Steps: First, Do No Extrapolation. *Diabetes Care* **2020**;
9 43:2631-4.
- 10 44. Mukherjee R, Smith A, Sutton R. Covid-19-related pancreatic injury. *Br J Surg* **2020**; 107:e190.
- 11 45. de-Madaria E, Capurso G. COVID-19 and acute pancreatitis: examining the causality. *Nat Rev*
12 *Gastroenterol Hepatol* **2021**; 18:3-4.
- 13
14

1 **Figure Legends**

2 **Figure 1. The experimental scheme and the viral load, blood glucose levels, and**
3 **pathological changes in the pancreas of SARS-CoV-2-infected cats**

4 (A) Six cats were inoculated with 2×10^7 TCID₅₀ of SARS-CoV-2 via intratracheal and
5 intranasal administration on day 0; the cats were sacrificed at 3, 5, and 7 days post-
6 infection (dpi) to collect the tissue and blood samples. (B) The distribution of SARS-
7 CoV-2 in the primary organs of SARS-CoV-2-infected cats was evaluated using
8 quantitative real-time PCR. The major organs were harvested for the measurement of
9 viral loads at 3, 5, and 7 dpi. The values shown are means of the viral loads for the two
10 cats each euthanized at 3, 5 and 7 dpi. (C) Blood glucose levels of control and SARS-
11 CoV-2-infected cats at 3, 5, and 7 dpi. Each color bar represents the value from an
12 individual animal (3-1 and 3-2: SARS-CoV-2-infected cats at 3 dpi; 5-1 and 5-2: SARS-
13 CoV-2-infected cats at 5dpi; 7-1 and 7-2: SARS-CoV-2-infected cats at 7 dpi). Dashed
14 lines indicate the normal range of blood glucose (70-150 mg/dL). (D) Haematoxylin and
15 eosin-stained pancreatic tissue of cats challenged with SARS-CoV-2 at 5 dpi. Lesions
16 were absent in (a and b) the mock-infected and (c and d) challenged cats. Black bar, 200
17 μm . Green bar, 50 μm . (E) Immunohistochemical detection of SARS-CoV-2 NP antigen
18 at 5 dpi in the pancreatic islets of (a and b) mock-infected and (c and d) challenged cats.
19 Black bar, 200 μm . Green bar, 50 μm .

20

1 **Figure 2. Detection of SARS-CoV-2 nucleocapsid protein (NP), Spike protein, ACE2,**
2 **insulin (INS), and glucagon (GCG) in the pancreatic tissues of cats infected with**
3 **SARS-CoV-2**

4 (A1-A4) Representative pancreatic tissue sections from cats infected with SARS-CoV-2
5 with staining for SARS-CoV-2 NP (orange), INS (red), and GCG (green) and with DAPI
6 (blue). Scale bars, 400 μm . (B1-B4) Representative pancreatic tissue sections from cats
7 infected with SARS-CoV-2 with staining for SARS-CoV-2 Spike protein (red), INS
8 (orange), GCG (green) and with DAPI (blue). Scale bars, 200 μm . (C1-C4)
9 Representative pancreatic tissue sections from cats infected with SARS-CoV-2 with
10 staining for SARS-CoV-2 NP (orange), ACE2 (red), and GCG (green) and with DAPI
11 (blue). Scale bars, 200 μm . (D1-D4) Representative pancreatic tissue sections from
12 mock-infected control cats with staining for SARS-CoV-2 NP (orange), INS (red), and
13 GCG (green) and with DAPI (blue). Scale bars, 200 μm .

14
15 **Figure 3. Cats immunised with the inactivated virus were resistant to subsequent**
16 **infection and hyperglycaemia**

17 (A) Nine sub-adult cats (immunised cats (n = 6); normal control cats (n = 3)) were
18 intranasally infected the virus at 2×10^7 TCID₅₀ and euthanised at 3, 5, and 7 dpi to
19 collect tissue and blood samples. (B) The serum neutralising anti-SARS-CoV-2 antibody
20 titres were measured in Vero cells after immunisation (n = 6). The dotted line indicates
21 the detection limit (serum neutralising antibody titre = 1:20). (C) The blood glucose

1 levels were measured at 3, 5, and 7 dpi. Each color bar represents the value from an
2 individual animal (IM3-1 and IM3-2: Immunized and SARS-CoV-2-infected cats at 3
3 dpi; IM5-1 and IM5-2: Immunized and SARS-CoV-2-infected cats at 5dpi; IM7-1 and
4 IM7-2: Immunized and SARS-CoV-2-infected cats at 7 dpi; no-IM3: Non-immunized
5 and SARS-CoV-2-infected cats at 3 dpi; no-IM5: Non-immunized and SARS-CoV-2-
6 infected cats at 5 dpi; no-IM7: Non-immunized and SARS-CoV-2-infected cats at 7 dpi;).
7 Dashed lines indicate the normal range of blood glucose (70-150 mg/dL).

8

ACCEPTED MANUSCRIPT

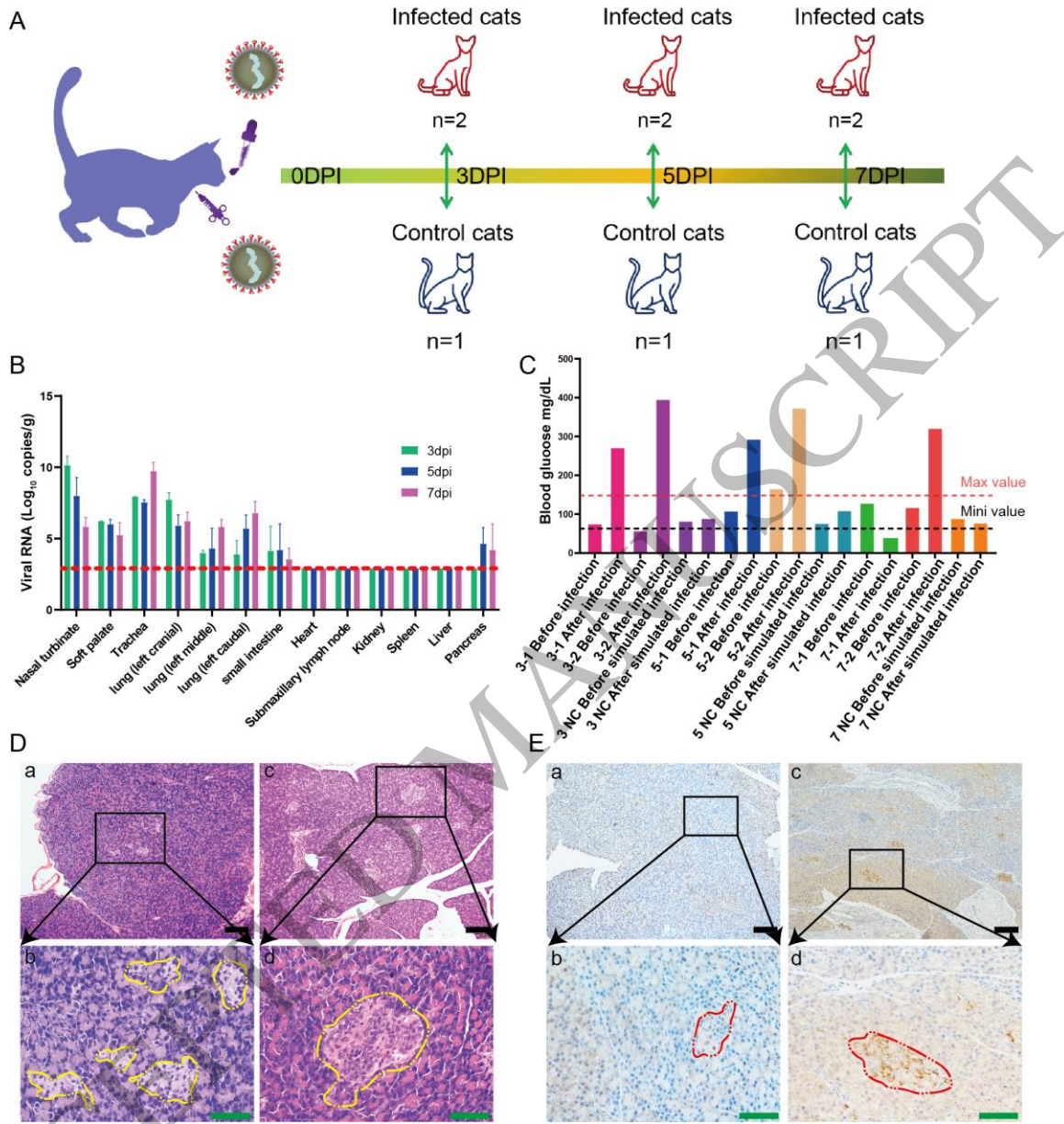
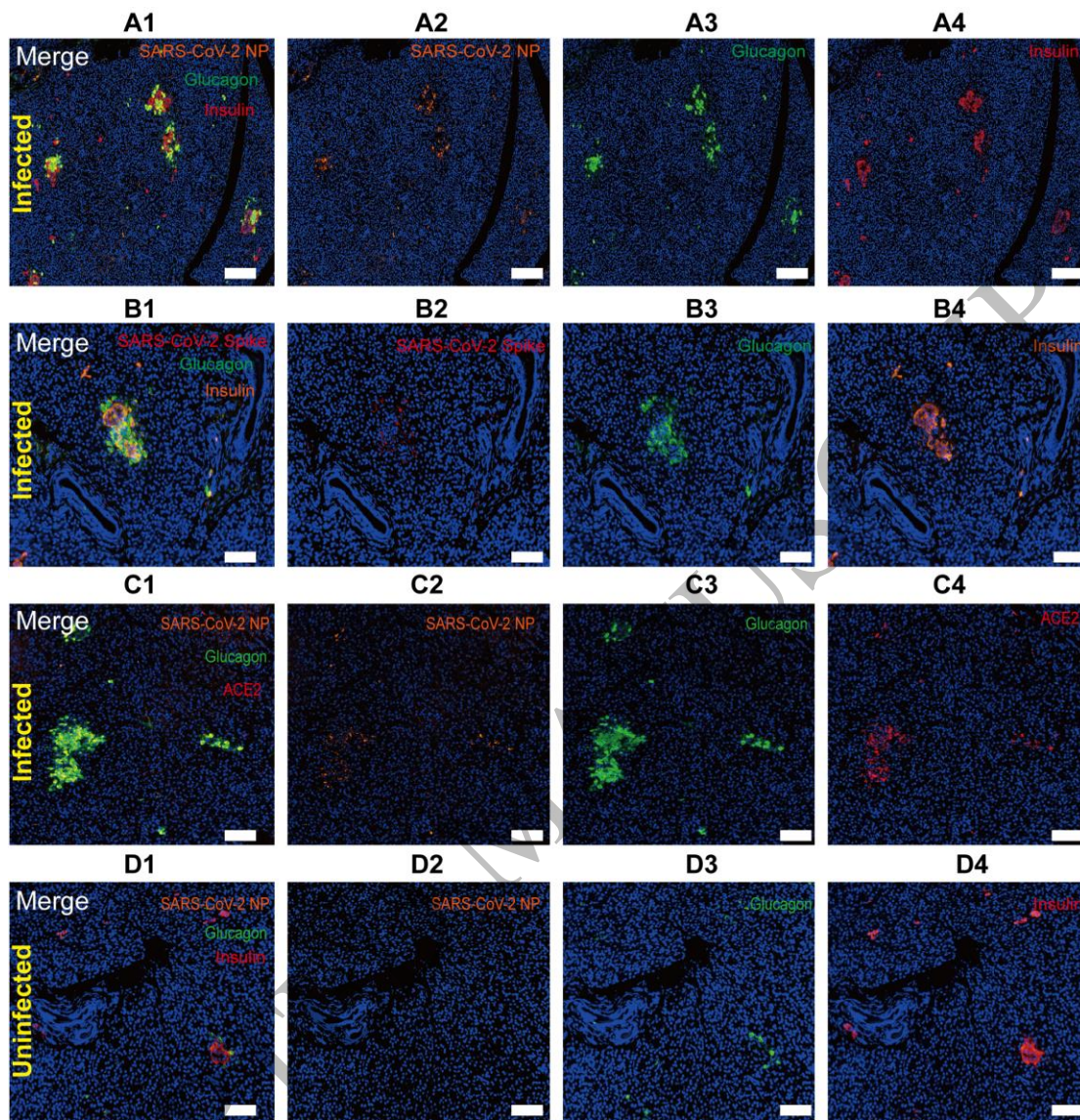


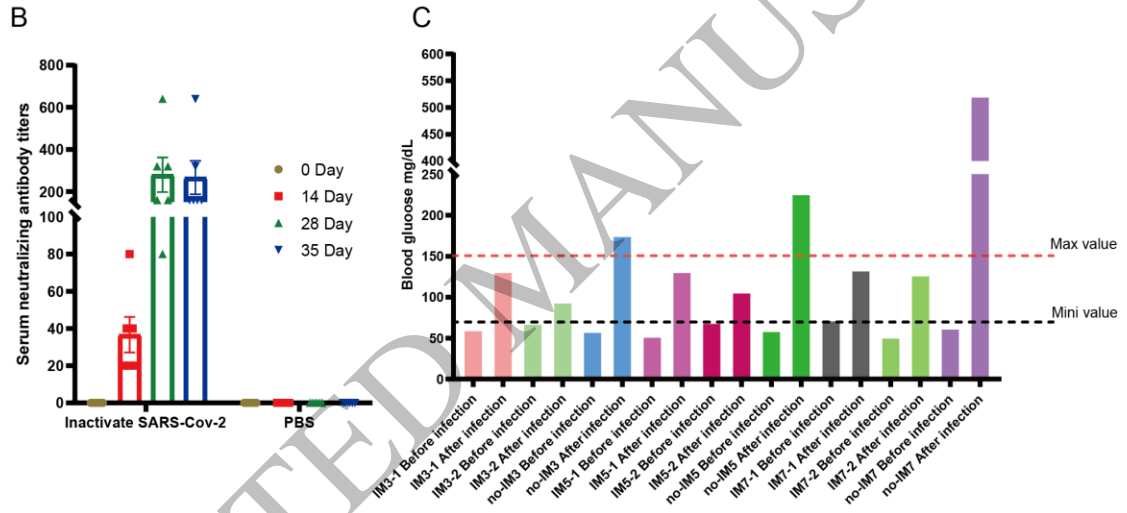
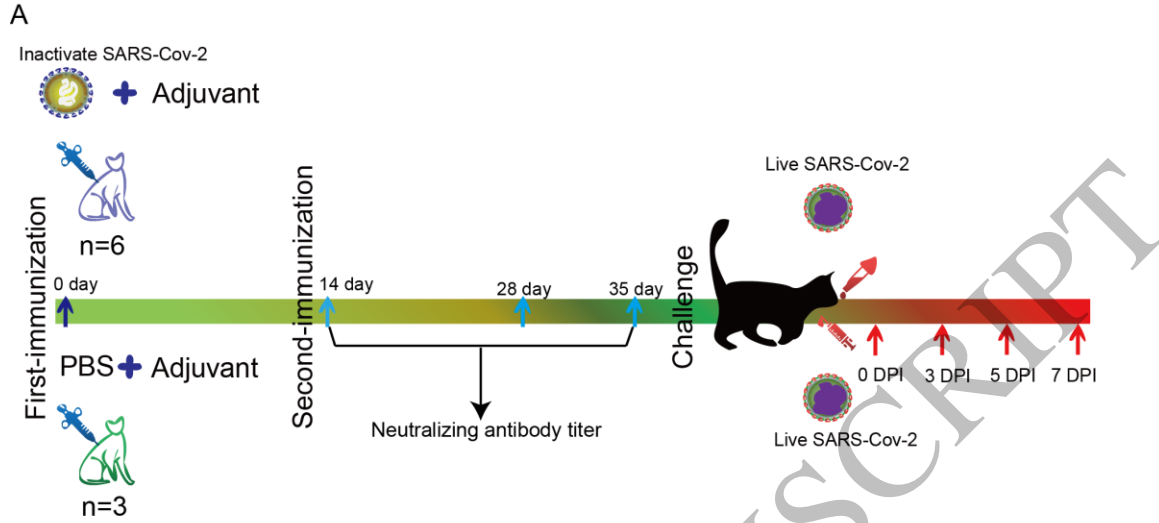
Figure 1
147x162 mm (4.2 x DPI)

1
2
3
4



1
2
3
4

Figure 2
147x154 mm (4.2 x DPI)



1
2
3

Figure 3
147x144 mm (4.2 x DPI)